Proceedings of the 21st ICSMGE, Vienna, Austria, 14 – 19 June 2026. Pistrol, Adam & Schweiger (eds.)
Published by: ÖGG, Austrian Society for Geomechanics, Salzburg, Austria, ISBN 978-3-9503898-4-5
https://doi.org/10.53243/ICSMGE2026-593

Ballast stiffness estimation based on measurements during dynamic track stabilization

Manuel Dafert, Johannes Pistrol, Dietmar Adam
Institute of Geotechnics, TU Wien, Austria, manuel.dafert@tuwien.ac.at

Fritz Kopf
FCP – Fritsch, Chiari & Partner ZT GmbH, Vienna, Austria

ABSTRACT: The Dynamic Track Stabilizer (DTS) is used to compact the ballast after track tamping. Ballast compaction with the DTS is known to increase the lateral track resistance and thus the (shear) stiffness of the ballast. The shear stiffness of railway ballast can be expressed as a strain dependent shear modulus *G*. The conducted research yielded two approaches for estimating the shear modulus of ballast, which are based on measurements taken during dynamic track stabilization. Firstly, the Hardin equation, with its enhancement for coarse-grained soils, is used to estimate the small strain shear modulus for a given grain size distribution curve. This provides a foundation for estimating shear modulus degradation curves (G/G_{max}). These curves are calculated by measuring ballast shear strains with accelerometers at the top and bottom of the ballast layer, as well as the stress distribution within the ballast layer. For a specific track section, different shear strains and stresses are observed for a bypassing DTS, resulting in the aforementioned shear modulus degradation curves. The results of a regular maintenance operations demonstrate that these shear modulus degradation curves align with those described by other researchers for similar material. Secondly, a SDOF model was developed to analyze the track-ballast interaction under harmonic loading, which is caused by the dynamic track stabilizer. For this model, the mass and mass moment of inertia of the track and the geometry of an equivalent machine foundation are estimated using influence lines, with spring and dashpot coefficients according to the Hall analog. Furthermore, the model response is fitted to the field test data using an optimization algorithm. The resulting shear moduli show plausible values for both loose and compacted ballast conditions. Consequently, this method can serve as the basis for an Intelligent Compaction (IC) system with the DTS in the future.

KEYWORDS: Soil Dynamics, Ballast Compaction, Railway Track, Track Stiffness, Machine Soil Interaction.

1 INTRODUCTION

Ballast compaction with the Dynamic Track Stabilizer (DTS) after track tamping operations is usually considered beneficial for the following track properties:

- Lateral track resistance
- Durability of track geometry
- Elastic and dissipative track behavior

Many researchers have proven the positive influence of ballast compaction on lateral track resistance (Feurig, 2020). However, a significant influence on vertical track resistance and, consequently, on the durability of track maintenance operations is expected but has not yet been demonstrated. Similarly, there are no significant findings regarding the influence of ballast compaction on the elasticity and energy dissipation of railway tracks.

All these properties are influenced to some extent by the elasticity of the track ballast (Li et al., 2015; Khatibi, Esmaeili and Mohammadzadeh, 2017). However, in railway engineering, (vertical) track stiffness is typically considered in the context of an infinite, continuously elastically supported beam model. This stiffness is governed by the flexural rigidity of the track, which is provided by the rails, fasteners, and sleepers, as well as the modulus of subgrade reaction. The modulus of subgrade reaction reflects the stiffness of all granular layers, including the track ballast, subballast (if applicable), and subgrade. Therefore, track stiffness is often considered a measure of track quality, with higher values typically indicating a better track foundation (Li et al., 2015).

There are several methods for (continuously) measuring the overall track stiffness (Tong et al., 2022). However, to the authors' knowledge, none of these methods provide continuous measurements of the granular layers' crucial stiffness conditions. The individual stiffness of the granular layers can either be found by in situ testing procedures or by laboratory tests.

Regarding in situ testing, there is no standardized method for assessing the stiffness of the ballast layer. However, a previous study by Lamas-Lopez et al. (2016) on a French railway track examined results from measurements with the light dynamic penetrometer (PANDA) and the light falling weight deflectometer. According to the study, both methods produced reproducible results for all layers in the case of the PANDA test, but only for the ballast layer in the case of the light falling weight deflectometer.

For laboratory testing, the use of large-scale triaxial tests is considered state-of-the-art for analyzing the stress-strain behavior of granular material in detail, especially in the context of ballast. Extensive research on the (soil-)mechanics of ballasted railway tracks was performed by Indraratna and his team. Their laboratory tests indicate that the resilient modulus of ballast depends on the confining pressure, and that the resilient modulus of loose ballast increases with increasing load cycles until 100,000 cycles. After that point, no further increase of the resilient modulus can be observed (Indraratna, Lackenby and Christie, 2005). Additionally, Sun, Indraratna and Ngo, (2018) discussed the dependence of the resilient modulus on the loading frequency. After surpassing a critical frequency dependent on confining pressure, ballast shows strain softening, indicating a reduced resilient modulus at higher loading frequencies.

However, there is currently no in-situ procedure for measuring shear modulus degradation curves of the ballast layer. The objective of the research presented is to contribute to resolving this issue by describing an in-situ procedure for calculating the shear modulus of the ballast layer when subjected to different shear strains induced by the dynamic track stabilizer. Additionally, a framework is presented for developing a continuous stiffness estimation of the ballast layer based on measurements on the dynamic track stabilizer (Dafert et al., 2024).

2 DATA BASE

This study is based on measured data from two different locations. The first data set (further referred to as track A) was gained by observing a regular maintenance operation (tamping and stabilization) close to the town of Retz in July 2021. This section was originally equipped with a pressure cell and an accelerometer at the bottom of both, the ballast layer and the subballast layer during formation rehabilitation in July 2020 to collect data for future sub-ballast optimization (Kopf and Stern, 2022). During maintenance operations in 2021, accelerations and vertical stresses were monitored at the bottom of the ballast and subballast. Additionally, the acceleration of the sleeper positioned directly above the granular layers' accelerometers, as well as the bypassing DTS accelerations, were monitored. Additionally, the phase of the horizontal excitation force caused by the DTS was measured using inductive proximity sensors, and the position of the DTS was tracked with a GPS antenna. The process parameters of the DTS remained constant: an excitation frequency of 30 Hz, 40% of the maximum imbalance eccentricity, vertical loading of 134 kN, and an operating speed of 700 m/h. The grain size distribution of the ballast had already been analyzed by project partners. The full measurement setup is shown in the left part of Figure 1.

The second data set (further referred to as track B) was produced during a test campaign conducted in an Austrian Railways test facility (openrail lab, ÖBB) close to the town of Oberwart in October 2019. The following tests were performed using a 09-4X E3 tamping machine with two integrated and synchronized dynamic track stabilizing machines (both vibrating with the same phase), working directly behind each other:

- **Initial test run** – The DTS passes the metrologically equipped section without tamping, under in situ ballast conditions. The tamping operation is performed without track stabilization (DTS is switched off).
- **First test run** – the DTS passes the section (without tamping) after tamping (loose ballast).
- **Second test run** – the DTS passes the section (without tamping) a second time after tamping (compacted ballast).

The DTS process parameters remained constant throughout the tests (33 Hz excitation frequency, 100% of maximum imbalance eccentricity, vertical loading of 134 kN, operating speed of 2000 m/h). Therefore, it is possible to compare dense and less dense ballast conditions after tamping. The measurement setup included three-dimensional accelerometers on one (stationary) sleeper and on the DTS, as well as one-dimensional accelerometers to monitor vertical acceleration of the machine frame. Additionally, inductive proximity sensors measured the phase of the excitation force caused by the rotating imbalances of the DTS. Again, the DTS position was monitored during the tests using a GPS antenna. The full measurement setup is shown in the right part of Figure 1.

The two sites differed in terms of their superstructure and ballast. Track A near Retz had a modern superstructure with UIC 60 rails, concrete sleepers (spacing of 60 cm), a direct screw assembly fastening system, under sleeper pads, clean ballast conditions, and a subballast layer. In contrast, track B near Oberwart had an older superstructure with S 49 rails, wooden sleepers (spacing of 68 cm), and a direct screw assembly fastening system. It also had rather dirty ballast conditions and lacked a subballast layer.

Consequently, the two tracks exhibited different motion behaviors when excited by the DTS, as depicted in Figure 2. While the new track exhibited small rotations and mostly horizontal motion, the older track rotated almost simultaneously with horizontal translation. This can be described by calculating the vertical distance between the accelerometers on top of the sleeper and the position of the instantaneous center of rotation (for details see Dafert et al. (2024)). The instantaneous center of rotation has an almost constant distance to the accelerometers for the older track B and a small phase delay between rotational and translational motion. However, this distance varies greatly for the new track A, resulting in a phase delay of almost 90° between rotational and translational motion.

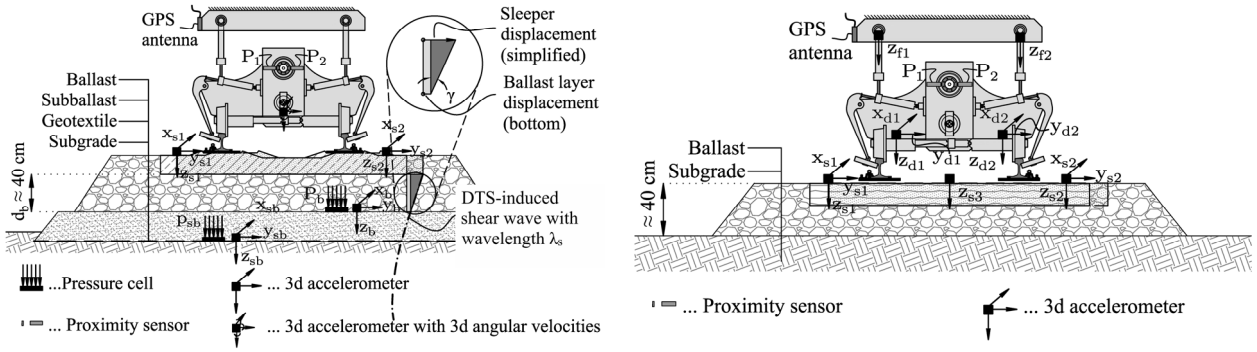

Figure 1. Left: Overview of measurement setup used at track A (modern track). Right: Overview of measurement setup used at track B (older track).

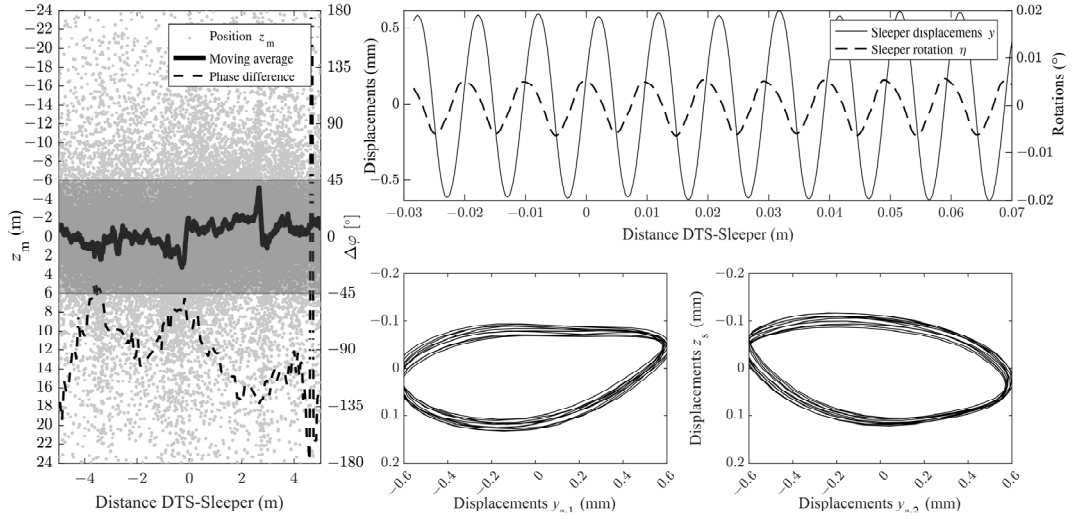

(a)

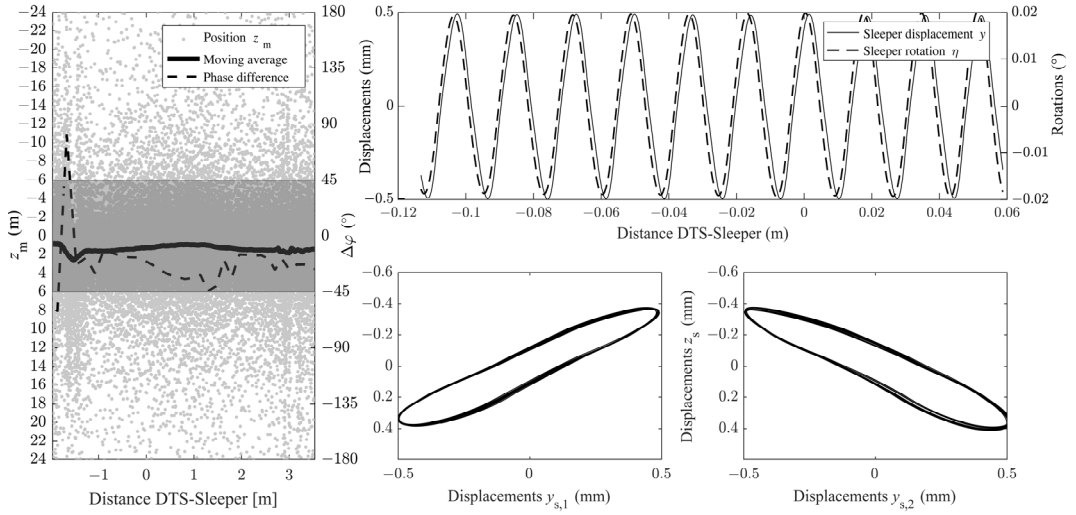

(b)

Figure 2. Left: Instantaneous center of rotation for a modern structure from track A (a) and an old structure from track B (b) with shaded areas highlighting phase differences between rotation and translation with less than 45°. Right: detailed plot for the measured displacement and rotation signal for the DTS above the monitored sleeper with sleeper motion in the y-z-plane beneath.

3 TRACK A – BALLAST SHEAR STRAINS AND SHEAR MODULUS DEGRADATION CURVES

The horizontal motion of the sleepers (see Figure 2) predominantly induces shear strains in the ballast layer in the y-z plane. When a DTS bypasses a fixed location, different amplitudes of these shear strains may be observed. These strains can be calculated using the measurement setup shown in Figure 1.

A

(1)

Equation (1) represents linearly decreasing deformations between the lateral displacements of the sleeper (with a mean value of $\bar{y}_s$ from the two three-dimensional sleeper sensors) and the lateral displacement y_b measured at the bottom of the ballast. The assumption of a linear shear deformation of the ballast layer is applicable because the wavelength of the induced shear wave is much longer than the ballast layer's thickness (Dafert et al., 2024).

The vertical stresses at the bottom of the ballast layer (as shown in Figure 1) were also monitored during the stabilization operation. Given the vertical stresses, the horizontal in situ stresses may be estimated by assuming earth pressure at rest for cohesionless soils (K0 = 1 – sin(Φ)). With known shear strains and stress state, shear modulus degradation curves can be calculated using an alternative of the Hardin-Drnevich formulation developed by Wichtmann and Triantafyllidis (2013):

(2)

Where a is a curve-fitting parameter which depends on the uniformity coefficient C_u, p is the mean confining pressure, and p_{atm}=100 kPa is the atmospheric pressure. However, for calculating the degradation curves, the shear modulus for small strains G_{max} needs to be estimated (or tested) first. Within the present research, an empirical formula for estimating the small strain shear modulus of coarse-grained soils developed by Hardin and Kalinski (2005) is used:

(3)

Where OCR is the overconsolidation ratio (for clean ballast OCR=1), k is a constant factor, e is the void ratio, $f(D)$ is a scalar function governed by the grain size distribution and the stress state, S is the stress coefficient, v is the elastic Poisson's ratio, n = 0.5 is an elastic constant that is the same for all types

of soil, and σ_v and σ_h are the vertical and the horizontal in situ stresses.

It is important to note that most input parameters for Equation (3) must be estimated. Therefore, a plausible range of values has been determined for these parameters, which are listed in Tab. 1 (for further details, see Dafert et al. (2024)).

Table 1. Range of (dimensionless) values for estimating G_{max}

Parameter	Range
Void ratio e	0.35 – 1.077
Stress coefficient S	1200 – 1700
Poisson's ratio ν	0.33
Earth pressure coefficient K_0	0.181 – 0.371

By inserting these values and the measured stresses and shear strains into Equation (2) and Equation (3), the shear modulus can be calculated with respect to the distance between the DTS and the monitored section (shown in Figure 3). Normalizing the obtained curve results in the graph shown in Figure 4, which is in accordance with the results from Hardin and Kalinski (2005).

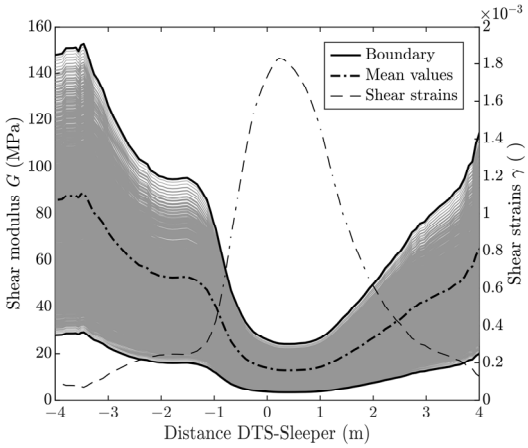

Figure 3. Shear modulus degradation curves derived from (implicit) measurements of shear strains and vertical pressures.

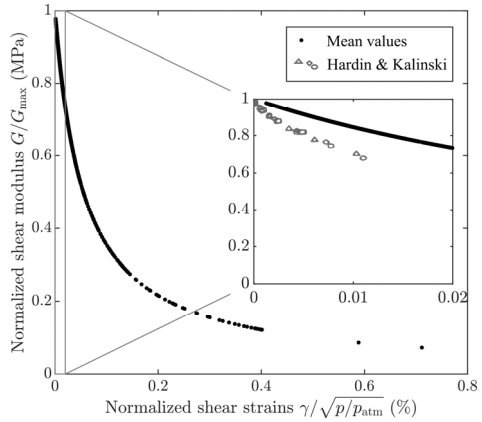

Figure 4. Normalized shear modulus degradation curve compared to results from literature.

4 TRACK B – FRAMEWORK FOR AN IC SYSTEM FOR THE DTS

Existing methods for estimating ballast stiffness do not provide continuous results along the railway line. This limitation could be overcome by developing a system for continuous stiffness estimation using the DTS. Comparable approaches have been successfully applied to vibratory rollers under the concepts of Intelligent Compaction (IC). These methods rely on monitoring the motion behavior of the compaction device, which is strongly influenced by the stiffness of the underlying material. When operating parameters such as excitation frequency, imbalance eccentricity, and vertical loading are kept constant, any deviations in motion behavior indicate changes in soil (or in case of the DTS ballast) stiffness.

4.1 *A simplified mechanical model for track-ballast-interaction under DTS excitation*

From a structural dynamics' perspective, dynamic track stabilization involves two interacting subsystems: the DTS and the track itself. Recent studies have shown that, due to the rigid design of the hydraulic cylinders of the DTS, the machine frame is also dynamically excited during operation. Therefore, both the ballast conditions (which can vary along the track due to subgrade differences, previous load history, or track geometry) and the machine frame properties (such as mass variation from equipment loading or differing frame designs between machines) must be considered in a mechanical model representing the DTS in operation. Because the DTS introduces more variability than typical compaction devices, this study focuses on developing a simplified estimation approach based solely on the measured track motion. The aim is to evaluate its suitability for IC applications and to identify the main challenges for further development.

In this simplified model, the dynamic behavior of a track segment is represented as a harmonically loaded machine foundation. A horizontal harmonic force applied at the railhead induces both lateral translation and rotation, the latter arising from the force's eccentricity relative to the track's center of mass. Applying the law of conservation of momentum and impulse leads to a two-degree-of-freedom system, or in other words, a system of two coupled differential equations. However, as shown above, the motion of old tracks during stabilization operations can be approximated as a purely rotational movement about a (temporarily) constant instantaneous center of rotation. Thus, the governing equations can be rewritten into the familiar form of a single-degree-of-freedom (SDOF) oscillator by applying the law of conservation of momentum at this instantaneous center of rotation:

(4)

Figure 5 shows the kinetic and geometric properties used in Equation (4), in which the ballast reaction is represented by spring-dashpot elements. The mass moment of inertia used in Equation (4) is calculated as follows:

A

(5)

Index r denotes rail properties and index s denotes sleeper properties.

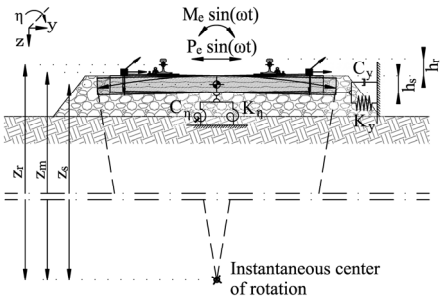

Figure 5. Geometric and kinetic properties required for Equation (4).

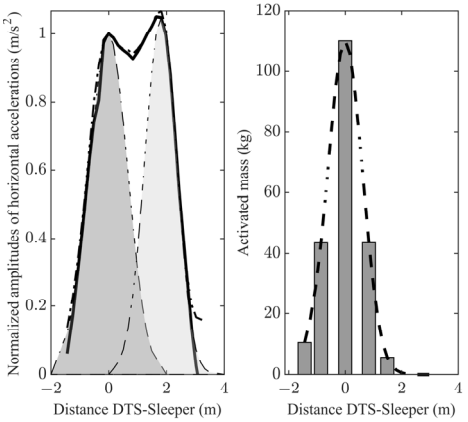

Figure 6. Left: Normalized amplitudes of horizontal accelerations (g(x)) for the initial test with derived influence areas of the monitored section (shaded areas). Right: Influence line for the sleeper masses with averaged normalized amplitudes (f(x)).

4.2 *Estimation of the mass moment of inertia of the SDOF-system*

Initially, the masses and mass moments of inertia of the track section exited by the DTS are unknown. These properties are determined using an approach analogous to influence lines commonly applied in civil engineering. Continuous measurements of an instrumented sleeper's motion provide both the amplitude and the phase of its response relative to the phase of the dynamic excitation generated by the DTS imbalance. By capturing this information for all positions of the DTS along the track, a continuous influence line describing the sleeper's response is obtained. Since the DTS induces both rotational and translational motion of the sleeper, two distinct influence lines are derived: one corresponding to lateral accelerations and relating to the activated masses and another corresponding to angular accelerations and relating to the activated mass moments of inertia.

Calculating these influence lines requires the use of a FFT of time windows of the analyzed signal (i.e. the lateral sleeper accelerations within ten full imbalance rotations of the DTS). Further, only the normalized amplitudes (division by the peak acceleration caused by the preceding DTS) at the excitation frequency are considered. Since two DTS were involved at stabilizing operations of track B, the section of the normalized amplitudes generated by the preceding DTS (see Figure 6) is flipped at its amplitude peak for creating the influence line. This procedure is also performed for the section created by the following DTS. These curves are averaged and the generated 'mean curve' is multiplied by (for example) the lumped masses of the sleepers, resulting in an influence line like the one shown in the right part of Figure 6, which represents the influence line of the dynamically activated sleeper mass.

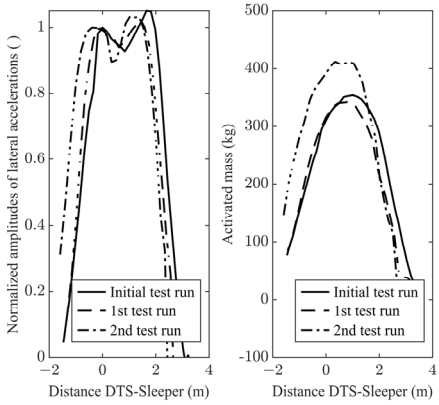

Figure 7. Left: Normalized amplitudes of lateral accelerations for all test runs. Right: Dynamically activated sleeper mass for all test runs.

A convolution integral is performed using this influence line (f(x)) and the normalized amplitudes (g(x)) to estimate the dynamically activated masses (or mass moments of inertia) at every instant when the DTS is close to the observed section:

A (6)

χ in Equation (6) is a local representation of the x-axis (which indicates the position of the DTS along the track). Figure 7 shows the activated masses that were calculated using this methodology. The resulting mass moments of inertia can be found in Dafert et al. (2024).

4.3 *Back-calculation of ballast shear modulus based on monitored sleeper-motion*

Even with the estimated mass moment of inertia and measured accelerations of the track – which were processed into velocities and displacements using numerical integration with the trapezoidal rule and digital filters – the stiffness coefficient, damping coefficient, and excitation moment of Equation (4) remain unknown. A set of equations developed by Hall is used to calculate the stiffness and damping coefficients. These equations were originally developed for use with machine foundations and require knowledge of the foundation' s geometry, soil density, Poisson's ratio, and shear modulus.

Regarding the foundation geometry, a rectangular foundation with the same height and width as a single sleeper but with a different length was assumed. The length was estimated using the same procedure as for the masses. However, the corresponding motion quantity was displacement instead of acceleration. Furthermore, the Poisson's ratio and density values were estimated as constants, with values of $\nu = 0.33$ and $\rho = 1700$ kg/m³, respectively. Consequently, the only unknown parameters are the shear modulus of the ballast and the excitation moment caused by the DTS, resulting in one equation with two unknowns.

One way to address this problem is to use optimization algorithms. Within this research, a gradient-based optimization algorithm was used to perform a least-squares optimization of the steady-state solution of the differential Equation (4):

(7)

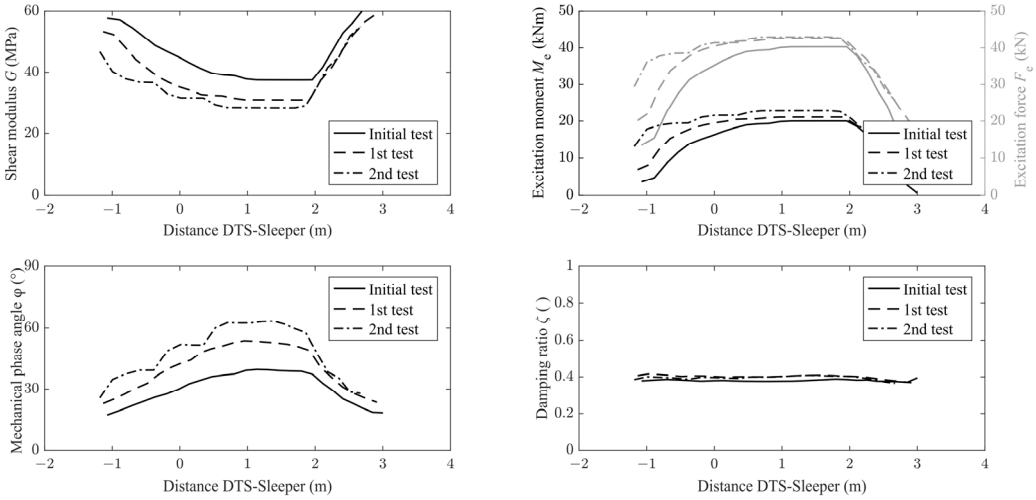

Figure 8. Shear modulus, mechanical phase angle, excitation force and moment, and damping ratio for the SDOF model with respect to DTS distance.

The error term S describes the difference between the measured signal, η, and the calculated signal, η^*, which represents the steady state solution of the SDOF problem with the mechanical phase angle φ_m, the damping ratio ζ, the excitation frequency ω and the undamped circular natural frequency ω_n. The optimization problem is solved within the same time windows, the mechanical properties (i.e. sleeper masses) have been calculated. Due to the existence of multiple local minima, the optimization problem is not sufficiently defined to obtain a unique solution. Consequently, the resulting shear modulus degradation curve highly depends on the initial values selected for the shear modulus, the excitation force, and the excitation moment. For the first time window, the following values were chosen as initial values: shear modulus $G = 50$ MN/m² (in accordance with the results from track A), excitation moment $M_e = 10$ kNm, excitation force $F_e = 25$ kN (approximately 20% of eccentric force caused by the rotating imbalances at 33 Hz). For the subsequent time windows, the results of the previous time windows were chosen as initial values for the optimization. The results of the optimization are shown in Figure 8.

5 OUTLOOK AND CONCLUSION

Two approaches for determining ballast shear modulus degradation curves were described based on measurements taken from two track sections: one modern (track A) and one old (track B) section, leading to the following conclusions:

- The presented measurement setup of the modern track is suitable to determine the shear strains and the vertical stresses of the ballast layer during dynamic track stabilization. Combining these measurements with empirical equations to estimate the small-strain shear modulus and (normalized) shear modulus degradation curves produces graphs that are consistent with results from the literature.
- It was shown that the motion of old tracks during dynamic track stabilization can be modeled as a SDOF system. The mass moment of inertia of this system can be estimated using an influence line inspired approach. The spring and dashpot coefficients of the SDOF system were linked with a model frequently used in soil dynamics – the Hall analog.
- The shear modulus, excitation force, and excitation moment were back-calculated using an optimization algorithm. The calculated shear modulus degradation curves showed higher values for the initial test than for subsequent tests after tamping, confirming the expected loosening due to the tamping process.

However, the calculated solution is not unique. Therefore, a dynamically decoupled DTS will be used to calculate the excitation forces and moments as rail reaction forces in future tests. This will ensure the uniqueness of the calculated solution. Additionally, a camera system will be used to continuously measure track movement. These measurements could be used to adjust the influence lines used to calculate the mass moments of inertia of the SDOF-system. This would enable continuous back-calculation of the shear modulus (evaluated at the point where the DTS is above the measurement section). The shear modulus could then serve as the basis for the first IC system for the DTS.

6 REFERENCES

Dafert, M., Pistrol, J., Kopf, F. and Adam, D., 2024. Ballast stiffness estimation based on measurements during dynamic track stabilization. *Proceedings of the Institution of Mechanical Engineers, Part F*, 238(10), 1269–1282.

Feurig, S., 2020. *Experimentelle und theoretische Untersuchungen zur Optimierung des Dynamischen Gleisstabilisators (DGS) im Hinblick auf eine Verbesserung der Gleislagestabilität.* TU München.

Hardin, B.O. and Kalinski, M.E., 2005. Estimating the Shear Modulus of Gravelly Soils. *Journal of Geotechnical and Geoenvironmental Engineering*, 131(7), 867–875.

Indraratna, B., Lackenby, J. and Christie, D., 2005. Effect of confining pressure on the degradation of ballast under cyclic loading. *Faculty of Engineering - Papers*, 55.

Khatibi, F., Esmaeili, M. and Mohammadzadeh, S., 2017. DEM analysis of railway track lateral resistance. *Soils and Foundations*, 57(4), 587–602.

Kopf, F. and Stern, J., 2022. Tragfähigkeitsmessungen am Unterbau der Eisenbahn. *ETR*, 71(6), 83–87.

Lamas-Lopez, F., Cui, Y.J., Costa D'Aguiar, S. and Calon, N., 2016. Geotechnical auscultation of a French conventional railway track-bed for maintenance purposes. *Soils and Foundations*, 56(2), 240–250.

Li, D., Hyslip, J., Sussmann, T. and Chrismer, S., 2015. *Railway Geotechnics*. 1. edn. London: CRC Press.

Sun, Q., Indraratna, B. and Ngo, T., 2018. Effect of increase in load and frequency on the resiliency of railway ballast. *Géotechnique*, 69

Tong, Y., Liu, G., Yousefian, K. and Jing, G., 2022. Track Vertical Stiffness – Value, Measurement Methods, Effective Parameters and Challenges: A review. *Transportation Geotechnics*, 37,

Wichtmann, T. and Triantafyllidis, T., 2013. Effect of Uniformity Coefficient on G/Gmax and Damping Ratio of Uniform to Well-Graded Quartz Sands. *Journal of Geotechnical and Geoenvironmental Engineering*, 139(1), 59–72.